Chapter 4

Studies on Cu/$ZrSiO_4$ surface composite fabricated by friction stir processing

As discussed earlier in chapter 1, to have good combination of properties such as strength, stiffness, ductility, toughness, hardness and wear resistance, conventional monolithic materials fall short. So to overcome these limitations and fulfil the ever increasing demands of properties, composites are getting popularity across the globe (Tjong and Ma, 2000) . Metal Matrix Composites (MMCs) have attracted attention globally due to combination of properties like high specific modulus and strength, enhanced elevated temperature properties, wear resistance and good abrasion resistance properties (Reddy et al., 2007, Anandatheerthan and Kumar, 2008). Because of the aforementioned properties, MMCs are being considered as good candidate for a wide range of applications in space shuttles, commercial airliners, electronic substrates, bicycles and automobiles (Das et al., 2007). Various reinforcements such as boron, silicon nitride, silica sand, magnesium oxide, mica, glass beads, boron nitride (Das et al., 2007), silicon carbide, titanium carbide, alumina, titanium boride, zirconium diboride and boron carbide (Das et al., 2009, Das et al., 2006) have been used as reinforcements for fabrication of MMCs. Although MMC reinforced with ceramics displays superior properties as compared to monolithic materials but due to higher processing cost its application is limited. The higher cost of MMCs can be reduced up to certain extent by using agricultural and industrial wastes as reinforcements in MMCs.

Among the above mentioned reinforcements, zircon sand is considered to be highly effective reinforcement because of its high refractoriness and resistance to sudden volume changes at elevated temperatures. Zircon possesses high melting temperature along with resistance to abrasion, impact and chemical attack (Pirkle and Podmeyer, 1998, Ezatpour et al., 2014, Banerji et al., 1983). It is being used by many researchers as reinforcement for manufacturing of MMCs and found to have

improved microstructural features, mechanical and tribological behavior (Das et al., 2006, Das et al., 2007, Das et al., 2009, Kumar et al., 2013, Panwar and Pandey, 2013, Gopi et al., 2013, Sharma and Das, 2009, Sucitharan et al., 2013, Panwar et al., 2014, Sharma et al., 2012, Abdizadeh et al., 2008, Pillai and Pandey, 1991, Li and Chao, 1996, Kumar et al., 2012, Okafor and Aigbodion, 2010, Sharma et al., 1999, Ejiofo et al., 1997, Abdizadeh et al., 2011, Kaur and Pandey, 2010, Kumar and Kailas, 2008) . To the best of our knowledge, there are no available reports on $Cu/ZrSiO_4$ surface composite fabricated by friction stir processing.

This chapter deals with the fabrication of $Cu/ZrSiO_4$ surface composite by reinforcing two different sizes of zircon particles in the copper matrix through friction stir processing route. Also, the effect of zirconia incorporation in the copper matrix has been assessed in terms of microstructural features, mechanical, tribological and electrical behaviour.

Chapter 4

Studies on $Cu/ZrSiO_4$ surface composite fabricated by friction stir processing

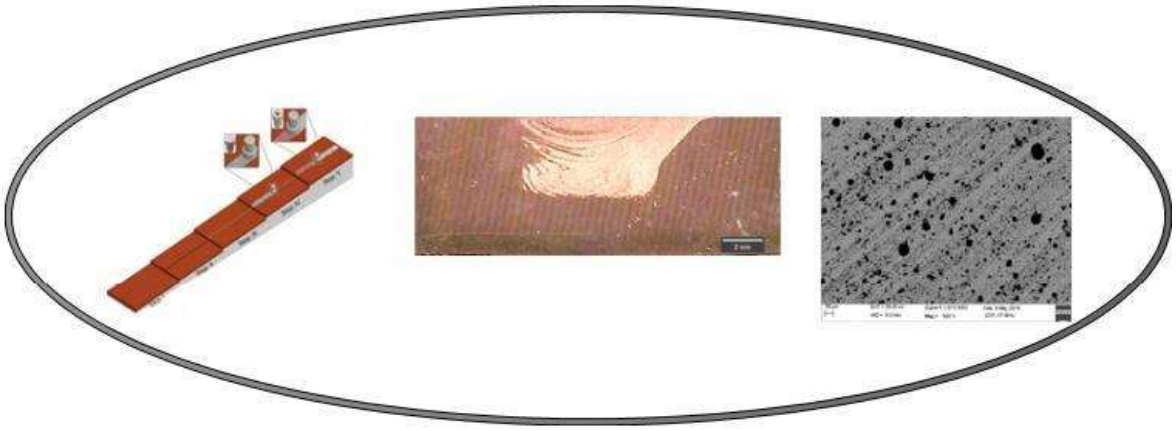

Results of this chapter have been published in

Kumar, H., Yusufzai, M.Z.K. and Vashista, M.(2018) 'Microstructure and Wear Behavior of Zircon Reinforced Copper Based Surface Composite Synthesized by Friction Stir Processing Route', Transaction of Indian Institute of Metals (2018) 71(8):2025–2033.

4.1 Introduction

This chapter focusses on the fabrication and characterisation of Cu/$ZrSiO_4$ surface composite fabricated by FSP. The microstructural features of the composite have been evaluated by optical microscopy, scanning electron microscopy and electron back scattered diffraction technique. The SZ of the composite was full of zircon particles with uniform and homogeneous distribution. The FSP and zircon particle incorporation in copper matrix led to fine and equiaxed grain structure of the composite. The interface between copper and zircon was interrupted at some places due to pores in case of larger zircon particles reinforcement whereas, interruption was not encountered in case of smaller sized zircon particles. The compositional analysis evaluated by XRD reveal no other phases except copper and zircon. The hardness, tensile strength and wear resistance of the composite was higher as compared to base copper and FSPed copper without reinforcement which was supposed to be due to the uniform dispersion of zirconia particle in the copper matrix and grain refinement. The ductility and electrical conductivity of the composite decreased with respect to base copper and FSPed copper without reinforcement.

4.2 Experimentation

4.2.1 Materials

Details of materials used along with their chemical compositions and particle size distributions are detailed in chapter 3, section 3.2.

4.2.2 Fabrication of Cu/$ZrSiO_4$ surface composite

The procedure followed for fabrication of surface composite (Cu/$ZrSiO_4$) via FSP in sequential form has been detailed in chapter 3, section 3.3.

4.2.3 Characterization of the Cu/$ZrSiO_4$ surface composite

Characterization methods employed for the present investigation include optical microscopy, scanning electron microscopy, electron back scattered diffraction, X-ray diffraction technique, microhardness, tensile testing, wear test and electrical conductivity measurement. The detailed procedures for all these characterizations are given in chapter 3, section 3.5.

4.3 Results and discussion

4.3.1 Macrostructure of the FSPed Cu/$ZrSiO_4$ composite

The macroscopic top view of the fabricated Cu/$ZrSiO_4$ surface composite is shown in Fig. 4.1, developed using the processing parameters rotational speed and a welding speed of value 1000 RPM and 40 mm/min.

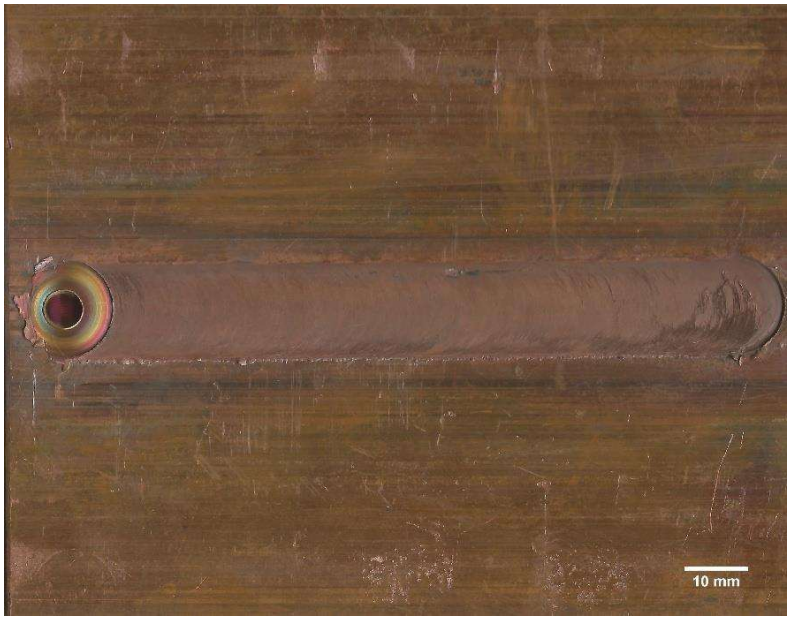

Figure 4. 1 Surface appearance of FSPed Cu/$ZrSiO_4$ surface composite

Various half-circled patterns which are characteristics of the FSPed plate having no depressions or discontinuities can be observed on the surface. Before conducting the final run at the aforementioned processing parameters, numerous trial runs were conducted to choose the optimized processing parameters for the production of the surface composite. The half-circled textures having no defects on the surface clearly validate the effectiveness of the chosen process parameters. The clean surface appearance with sound half-circled textures is necessary to produce defect-free composites by FSP. If there are any surface defects in the half-circled patterns, it will follow corresponding defects in the stir zone of the fabricated composite.

As tool rotates and travels during FSP, material temperature rises due to frictional heating and copper suffered severe plastic deformation. Thus the softened and then severely plasticized copper ahead the travelling tool shoulder was migrated from the front at the advancing side to the rear at the retreating side. This flowing

behaviour of the circle-form, softened band layer per rotation of tool shoulder led to the formation of the surface ring like textures. Fig. 4.2 describes the cross-sectional macrostructure of SZ of the fabricated Cu/$ZrSiO_4$ surface composite.

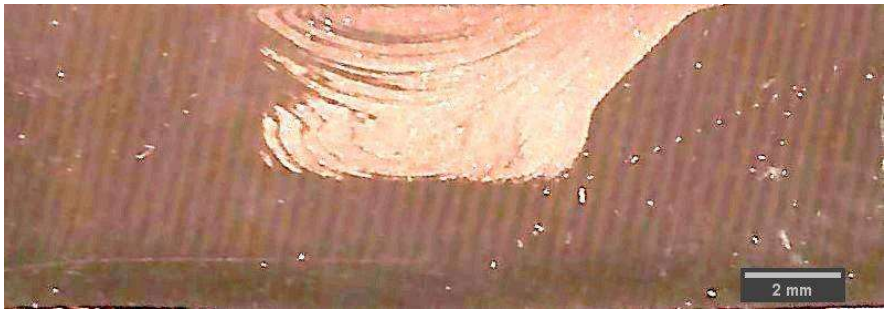

Figure 4. 2 Cross-sectional macrostructure of FSPed Cu/$ZrSiO_4$ surface composite

The grooves machined initially at the time of particle filling on the plate are not visible. Also, there are no macrostructure defects like tunnels and worm holes, evident from the SZ of FSPed composite, which clearly indicates the proper selection of process parameters in the present research work. This is due to the proper flow of sufficiently plasticized copper from advancing side of the tool to retreating side of the tool. The frictional heat generation between the specimen and rotating tool, can fully plasticize copper and propel them to flow violently, which transports the plasticized copper from advancing side to retreating side, causes the grooves to collapse and mixes the packed zircon sand particles with the plasticized copper and finally leading to the formation of the defect-free SZ, namely the Cu/$ZrSiO_4$ surface composite. It can be observed that the SZ resembles the basin like shape. In other words, the width of the SZ has reduced from the top surface to the bottom surface. The change in the width of the SZ from the top surface to the bottom surface may be attributed to the material flow during FSP.

During FSP two kinds of material flow exist namely: shoulder-driven flow and pin-driven flow (Rao et al., 2013). The material flow during FSP influenced by tool

shoulder up to certain depth while it is affected by tool pin below a certain depth. Hence, generally, in the case of, FSP of materials it is observed that the width of SZ reduces from the top surface to bottom surface. Besides these, it can be also observed that the SZ is asymmetrical about the rotational axis which is in agreement with the fact that generally in case of single pass FSP/FSW material tends to flow asymmetrically leads to asymmetry in the macrostructure of the SZ (Liu et al., 2014). This asymmetry of the macrostructure of SZ can be nullified by changing the rotational direction of the tool between consecutive passes of FSP as reported by various researchers (Dinaharan et al., 2017a). Various studies have been reported in which single passes of FSP resulted into symmetric macrostructure of SZ (Dinaharan et al., 2017c, Saravanakumar et al., 2017, Mahmoud et al., 2008).

4.3.2 The microstructure of the FSPed Cu/$ZrSiO_4$ composite

Figure 4.3 shows the optical micrograph of the fabricated Cu/zircon surface composite at various locations within SZ.

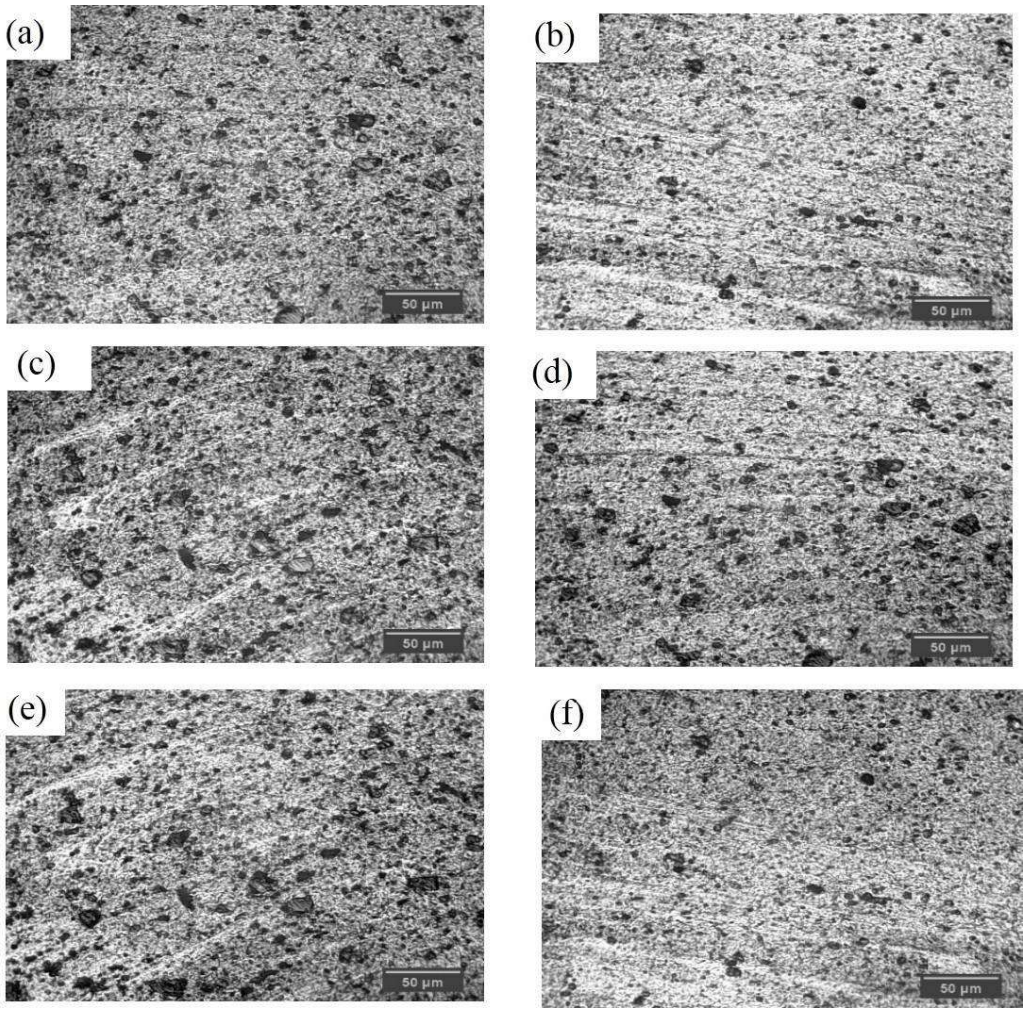

Figure 4. 3 Optical micrograph at various locations within SZ of the composite (a) towards advancing side at the top (b) towards retreating side on the top (a) at the center towards advancing side (d) at the center towards retreating side (e) towards advancing side at the bottom (f) towards retreating side on the bottom

It can be observed that the zircon particles are spread all over the SZ of the Cu/$ZrSiO_4$ surface composite. Furthermore, there is no concentration gradient of zircon sand i. e. no variation in zircon particle distribution is visible from advancing side to the retreating side or from the top side to the bottom side. Therefore, we can

safely conclude that zircon particle dispersion is almost constant throughout the stir zone under the investigated parameters. Results obtained in the present investigation for particle distribution contradicts the results reported by previous researchers (Sahraeinejad et al., 2015, Sathiskumar et al., 2013, Lekatou et al., 2015) where, they reported significant variation in particle distribution within SZ. The reason behind variation in the distribution of reinforcements was an insufficient flow of plasticized matrix strongly dependent on the plasticization level of the matrix and stirring action of the tool. In the present study, negligible variation in the dispersion of zircon particulates in the copper matrix was observed due to the mechanical action of the tool and sufficient plasticized copper flow. The viscosity of plasticized copper matrix during FSP was sufficient to restrict the free flow of zircon particulates in either direction. Thus concentration gradient of particulates was not observed in the fabricated surface composite as generally observed when composites are fabricated through any melt technique. The arc shaped feature at the left side of the macrograph in figure 4.2 indicates formation of onion rings. The onion rings encountered during FSP is supposed to be due to improper mixing of plasticized material in rotatory and vertical direction.

Fig. 4.4 shows SEM micrograph of the fabricated Cu/zircon surface composite at different magnifications. The micrographs clearly signify the nature of dispersion.

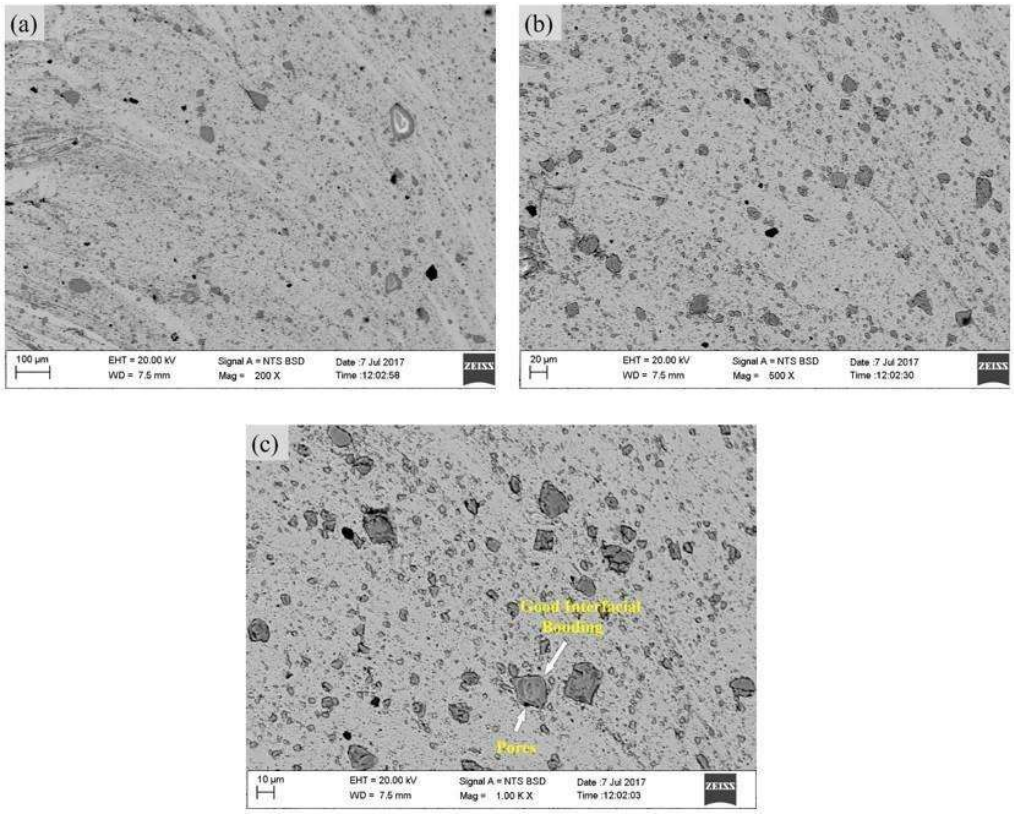

Figure 4. 4 SEM micrograph of SZ of the composite at different magnifications

The particles were scattered uniformly and homogenously. The entire area of SZ was filled with particles i.e. the particle-free zones were absent. The particles were fairly equidistant from each other. Grouping of particles or zero inter-particle distance region i.e. aggregation was not observed in the SZ. It could also be observed that the particles alignment along grain boundaries, known as grain boundary segregation was not evident in the micrographs.

In addition to particle distribution, the particle-matrix interface microstructure also plays an important role in determining the overall physical and mechanical properties of the FSPed particulate matrix composites (Akramifard et al., 2014). Therefore, it is imperative to study the Cu/Zircon interface microstructure in FSPed copper matrix composite in detail. So keeping that in mind, SEM micrograph of the fabricated Cu/zircon surface composite was taken at higher

magnification (Fig. 4.4 c) to reveal the nature of interface and bonding of filler with the matrix. It could be observed that the interface was interrupted at some portions due to porosity.

Friction stir processing led to the fracture of zircon particulates which led to the generation of sub sized particles of zircon sand. Fragmentation of zircon sand in the present investigation during FSP may be attributed to high plastic strain and vigorous rotating action of the tool. The combined action of these two factors led to fragmentation of zircon sand and hence reduction in the size of zircon sand. Also, the shape and size of the reinforced zircon sand played important role in its fragmentation. Due to the large size and uneven shape of zircon sand (Fig. 3.3), stress concentration happens at the sharp corners and finally led to fragmentation. Frictional heat developed during FSP is observed by reinforced particulates which act as a heat sink and thereby reducing the temperature of SZ and increased the flow stress and led to the fracture of reinforcements rather flow of the particulates.

The newly generated sub sized zircon particles had sharp edges and uneven shape as can be observed from Fig. 4.4. It can be observed from Fig. 4.4 (c) that copper was not properly adhered on the full surface of Zircon particulates. This led to the formation of some porous sites at the Cu/Zircon interface. This was attributed to uneven shape and sharp edges of zircon particulates as can be observed in Fig. 3.3 (a) due to which plasticized copper didn't fully flow over the surface of zircon particulates and led to the formation of porous sites at Cu/Zircon interface (Barmouz et al., 2011b, Dinaharan et al., 2017c).

As mentioned in the previous section there was an interruption at the copper/zircon interface due to porosity developed during FSP of Cu/$ZrSiO_4$ surface composite. Since the physical and mechanical properties of the composites depend

on the interface strength so to rectify the interruption encountered at the interface which was believed to be due to larger and uneven shape of the reinforced zircon sand, ball milling was used to reduce the size of zircon sand and make its surface even so that the interruption could be avoided at the interface during Cu/$ZrSiO_4$ surface composite fabrication. Fig. 4.5 shows the optical micrograph of the fabricated Cu/$ZrSiO_4$ composite at different locations of the SZ.

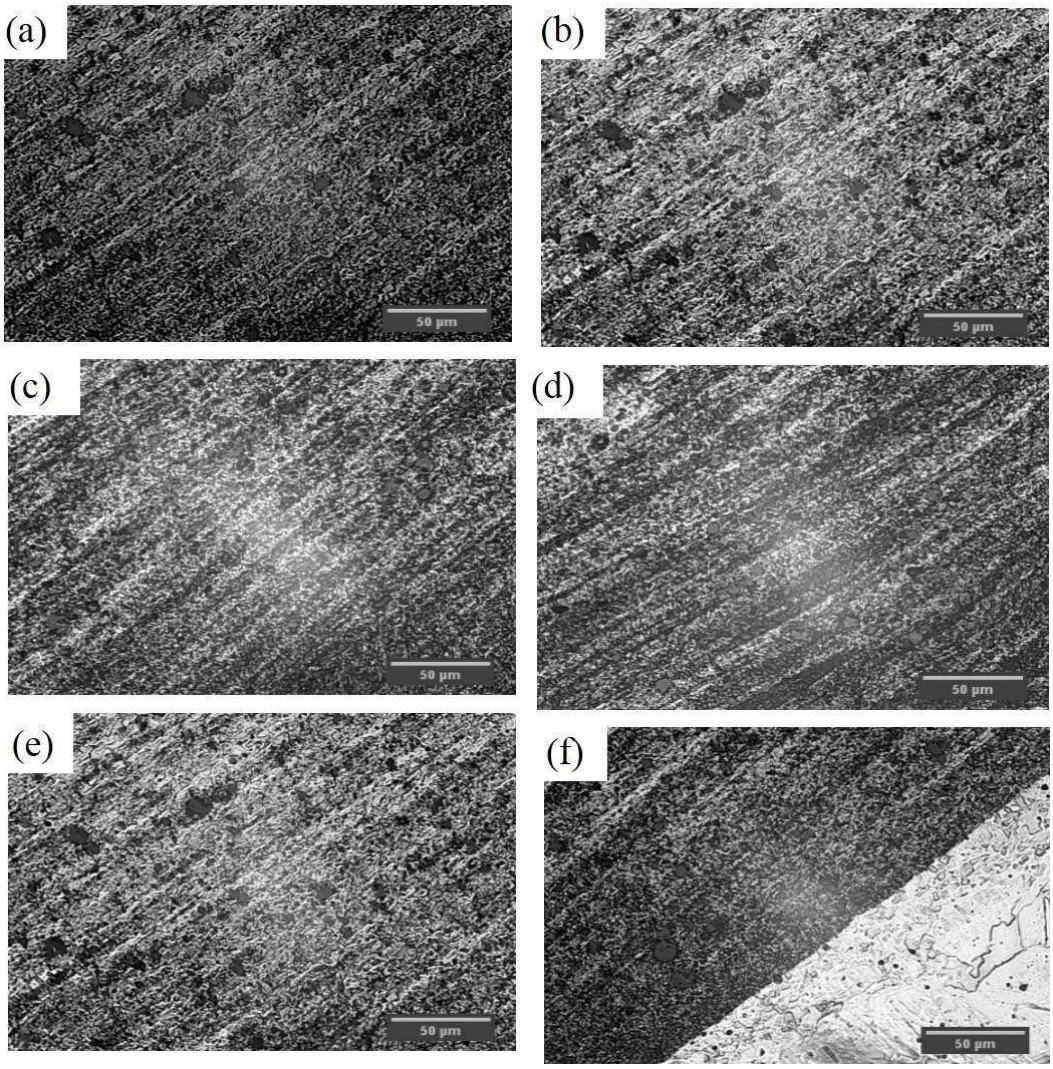

Figure 4. 5 Optical micrograph at various locations within SZ of the composite (a) towards advancing side at the top (b) towards retreating side on the top (a) at the center towards advancing side (d) at the center towards retreating side (e) towards advancing side at the bottom (f) towards retreating side on the bottom

The zircon particles are spread everywhere in the SZ and there is no variation in the particles distribution across SZ. The reason for uniform and homogeneous distribution of zircon particles are same as mentioned earlier in the case of larger particle size. Fig. 4.6 depicts SEM micrograph of the composite in SZ at higher magnification to have a better understanding of the Cu/zircon interface.

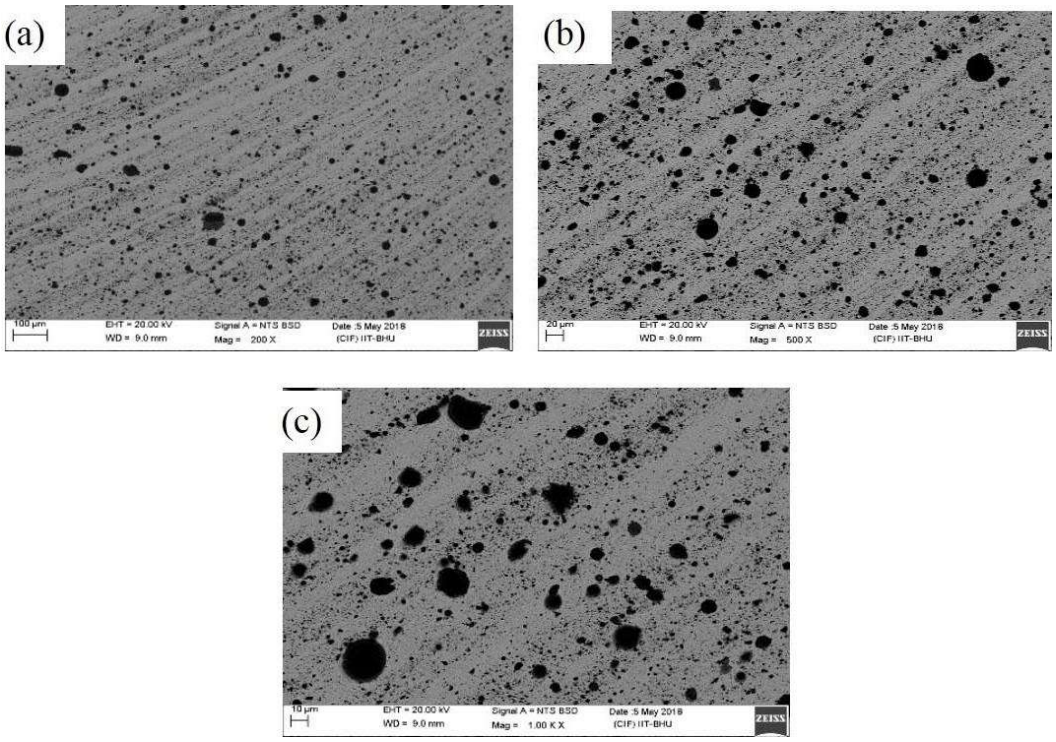

Figure 4. 6 SEM micrograph of SZ of the composite at different magnifications

It can be observed that there is no interruption at the interface and the composite showed good interfacial integrity without any pores. This is believed to be because of the smaller and smooth surface of the zircon sand which did not hinder the flow of plasticized copper. The severely plasticize copper spread all over the particulate and resulted into the un-interrupted interface without porosity.

By comparing Fig. 3.2 (a) and Fig. 4.6 (b), it can be observed that the zircon particles had not experienced size reduction during FSP, as the particle size of

zircon sand is almost the same before and after processing. In the present case, reinforced zircon particles were smaller in size and have smooth surfaces (Fig. 3.2 a) so they did not provide much resistance to flow of copper matrix and thus fragmentation did not happen. Moreover, the reinforced zircon had no sharp corners, so stress could not concentrate over there and fragmentation did not occur. Fig. 4.7 shows the grain structure of base copper and FSPed copper with and without reinforcement. It can be observed that base copper has coarse pancake-shaped grains.

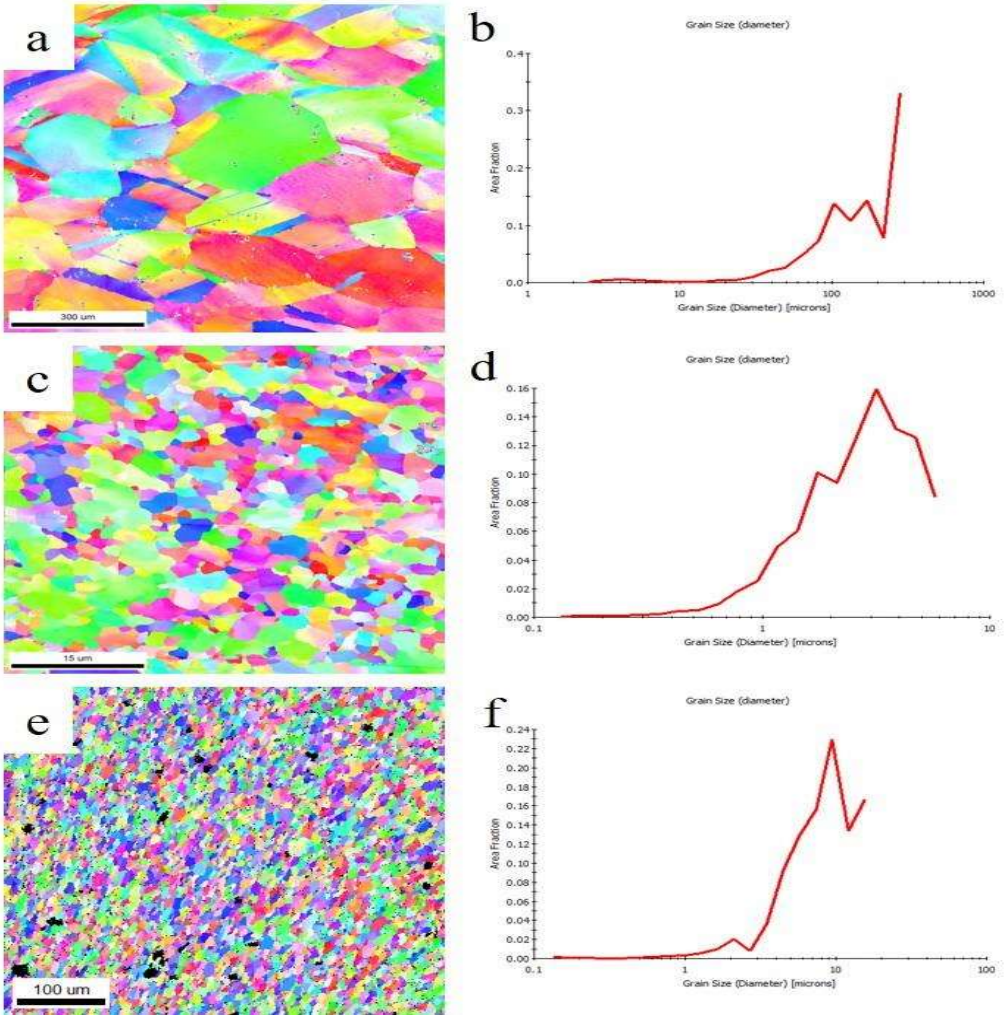

Figure 4.7 EBSD maps and corresponding grain size distribution of (a) and (b) base copper, (c) and (d) processed copper without reinforcement and (e) and (f) FSPed Cu/$ZrSiO_4$ composite

It can be observed that the coarse grain of base copper has transformed into fine and equiaxed grain after FSP without reinforcement. The estimated average grain size of base copper was about 107 μm. The grain size of base copper has reduced from 107 to 8 μm after a single pass of FSP. This much of drastic reduction in grain size of FSPed copper without reinforcement is believed to be due to dynamic recrystallization due to high strain rate and frictional heating (Mishra and Ma, 2005). Friction stir processing exhibits different types of recovery mechanisms such as continuous dynamic recrystallization, discontinuous dynamic recrystallization and geometric dynamic recrystallization (Ceriani and Verme, 2012). Due to the low stacking fault energy of copper, discontinuous dynamic recrystallization was main recovery mechanism. It can also be observed that the average grain size in case of FSPed Cu/$ZrSiO_4$ composite has further reduced. This was because of the uniformly distributed zircon particle in the copper matrix which hindered the growth of recrystallized grains due to the pinning effect.

4.3.3 Quantification of particle distribution of Cu/$ZrSiO_4$ composite

The quantification of dispersion uniformity was done using the Lorenz Curve by considering the spatial location and area of each individual zircon particle throughout the matrix. The image processing and data were acquired after binarizing the SEM image by ImageJ using quadrat method based on 20 equal sized quadrats having area 3161.95 μm^2 as shown in Fig. 4.8.

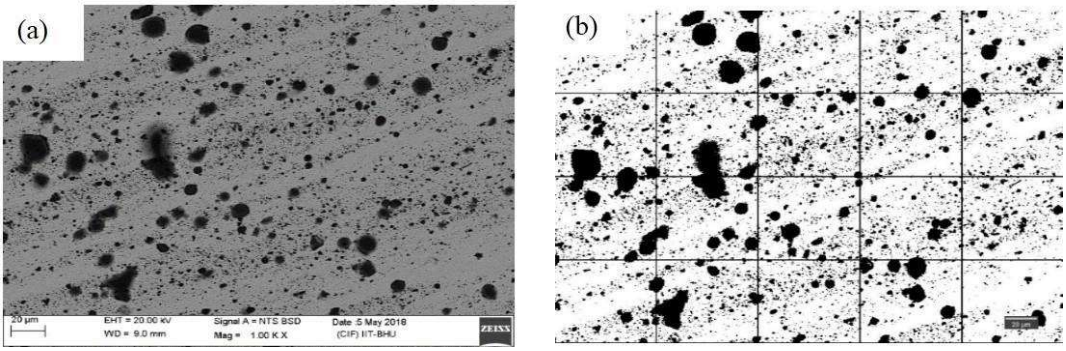

Figure 4. 8 SEM micrograph of fabricated composite Cu/$ZrSiO_4$ and its binarized image (b). The dark spots are Zircon particles and white spots are matrix

Also, the arithmetic mean of the area occupied by the zircon particles in each quadrat was calculated. The quantification of the degree of distribution and homogeneity was obtained by evaluating the relation between an equality line and the Lorenz curve representing the partial homogeneity (Ceriani and Verme, 2012). The homogeneity was calculated using the following equation:

$$\mathrm{H} = 1 - G$$

Where H is homogeneity and G is Gini Index (Rossi et al., 2014, Ding and Guo, 2001). The Gini Index was chosen for the calculations since it was conceived as a measurement of the distribution inequality of a given attribute. Since the value of the 'G' is related to the area below the Lorentz curve (A_L) by G = 1- $2A_L$, the homogeneity value is thus determined by H = $2A_L$. The quantification of particle distribution was evaluated through Lorentz Curve is shown in Fig. 4.9.

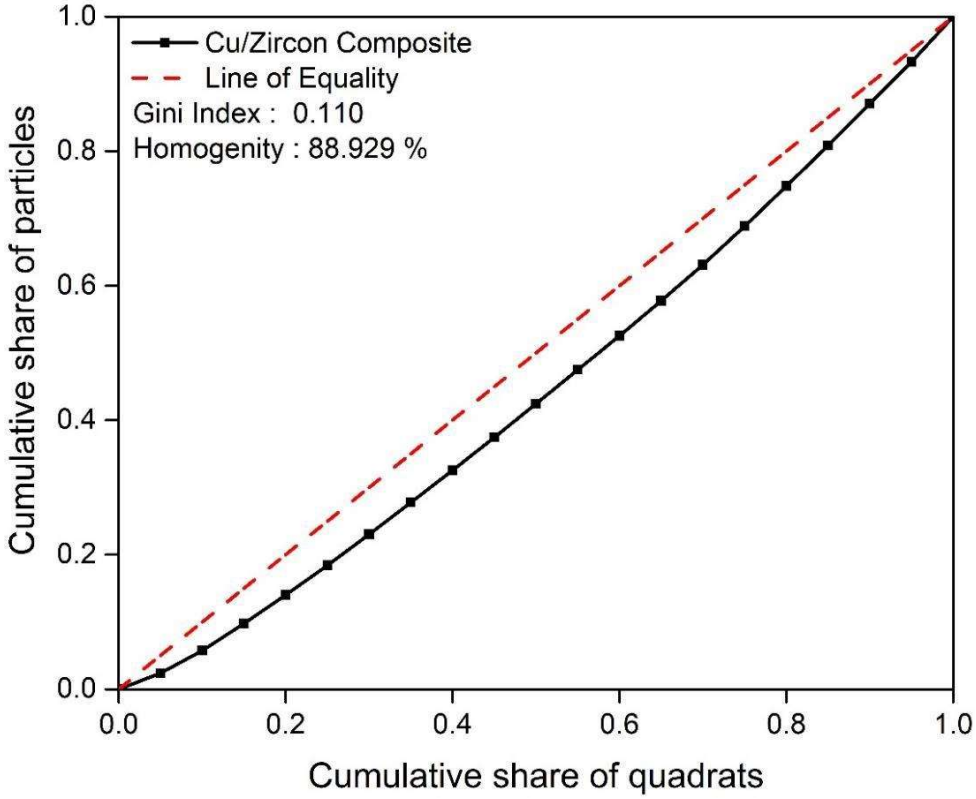

Figure 4. 9 Homogeneity curve for zircon particles

From Fig. 4.9, it is clear that the homogeneity curve for zircon particles is very close to the Line of Equality. The calculated Gini Index and homogeneity value for the present case were found to be 0.110 and 88.92% respectively. Which means zircon particles were dispersed almost uniformly in the copper matrix and were almost equidistant from each other.

Fig. 4.10 shows the XRD pattern of fabricated Cu/Zircon surface composite for detection of phases.

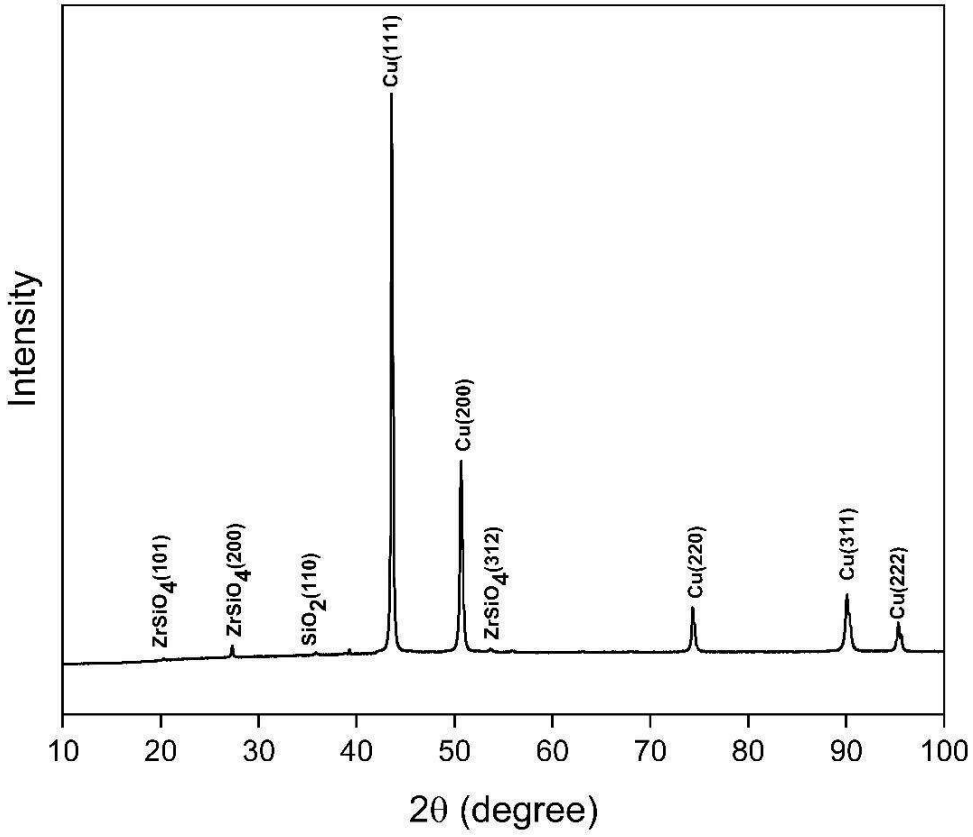

Figure 4. 10 XRD pattern of fabricated Cu/$ZrSiO_4$ surface composite

It could be observed that the peaks in the XRD pattern were only related to copper and zircon. The peaks related to any other compound or interfacial reaction products were not observed. The absence of intermetallics or in situ products in the XRD pattern of the fabricated composite is due to the development of insufficient heat during FSP to initiate a diffusion reaction due to the relatively short processing time and low processing temperature.

4.3.4 Mechanical properties of FSPed Cu/$ZrSiO_4$ surface composite

The mechanical performance of base copper, FSPed copper with and without reinforcement was assessed through Vickers microhardness and tensile testing. After tensile testing, the fractured samples were studied by using SEM analysis.

4.3.4.1 Microhardness

Fig. 4.11 shows the outcome of microhardness measurement on fabricated Cu/zircon surface composite.

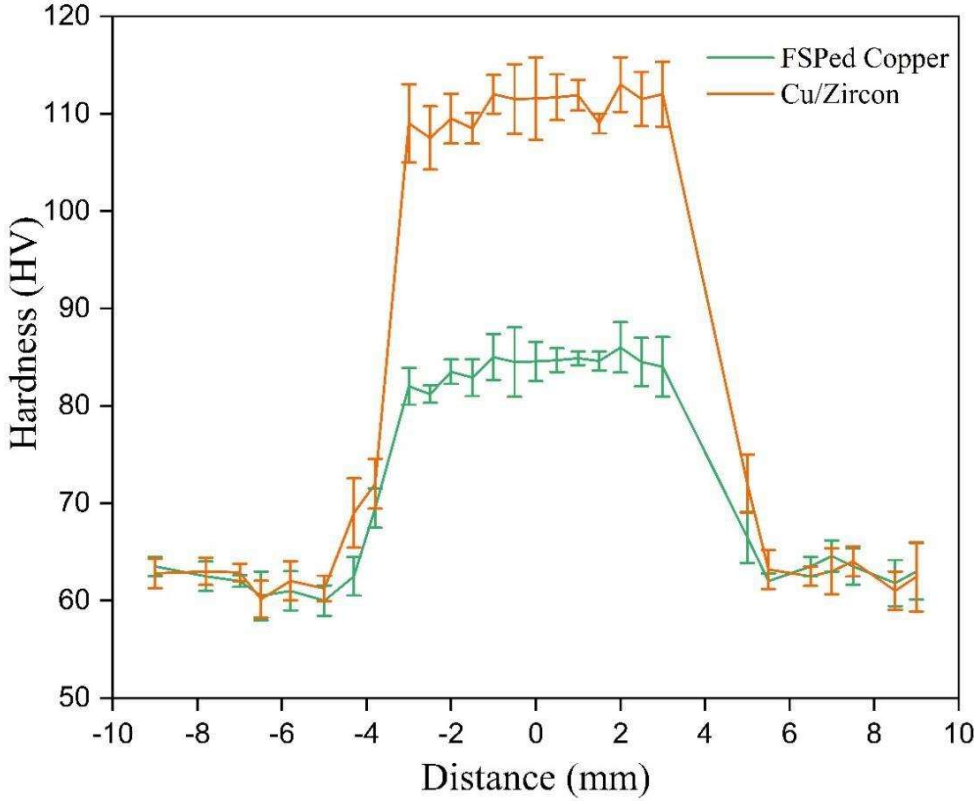

Figure 4. 11 Microhardness profile of FSPed copper with and without reinforcement

The profile of microhardness clearly shows that the hardness of the SZ improved significantly. The average hardness value of as received commercially pure copper

and fabricated Cu/zircon surface composite was estimated to be 67 HV and 110 HV respectively. The microhardness value of the FSPed copper without reinforcement has improved slightly in comparison of base copper. Dynamic recrystallization due to stirring action of pin led to decrease in grain size. Dynamic recrystallization also enhanced the generation of new dislocations due to plastic flow (Surekha and Els-Botes, 2011). The combined effect of reduction in grain size, generation of new dislocations and its pile up across grain boundaries led to increase in microhardness of SZ (Bauri et al., 2015). However, the increase in microhardness in case of the composite was more as compared to FSPed copper without reinforcement. This high value of microhardness in case of Cu/zircon surface composite as compared to friction stir processed copper was attributed to the pinning effect in the presence of zircon particulates, thermal mismatch and different deformation behaviour of copper and zircon particulates which generated additional dislocations (Lin et al., 2012). Zircon particulates were separated well in the copper matrix. Thus the pinning effect was intense which led to an increase in microhardness.

Besides these, the scattering of hardness values within the SZ of FSPed Cu/$ZrSiO_4$ composite was found to be minor, implying that the tool stirring efficiently dispersed the zircon particles in a reasonably uniform manner. Obviously, this is in absolute agreement with the microstructure analysis results (Fig. 4.3).

4.3.4.2 Tensile Properties

Stress-strain curves of the FSPed samples and the base copper are presented in Fig. 4.12.

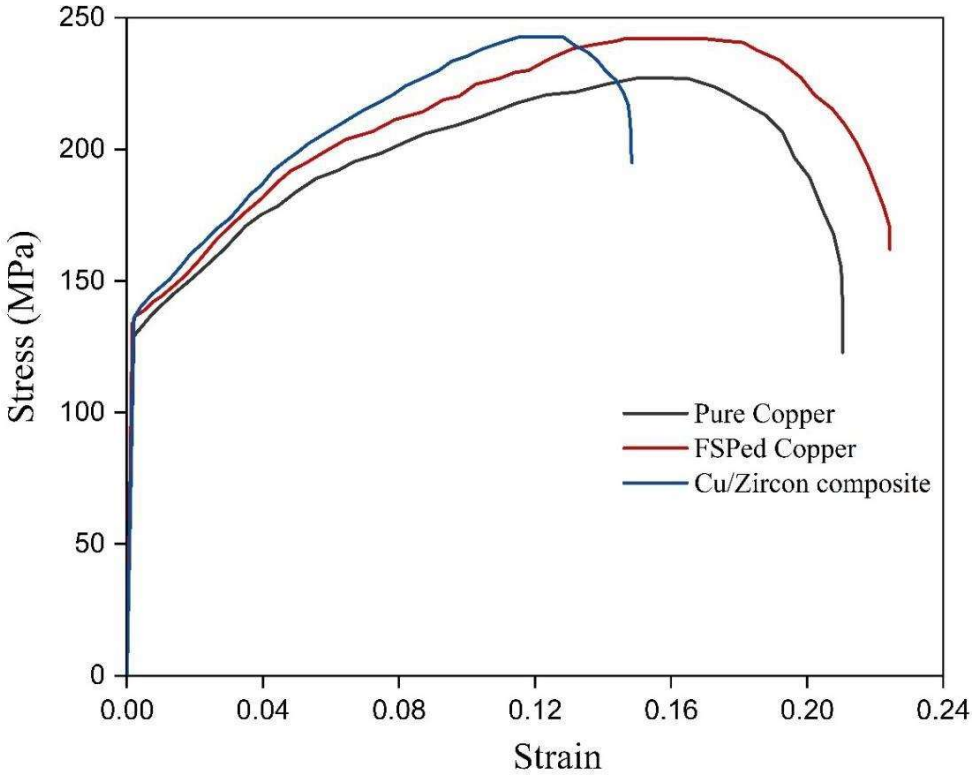

Figure 4. 12 Stress-strain curves of base copper, FSPed copper and FSPed composite

Clearly, compared with the tensile strength of the base copper, FSPed copper was slightly stronger. This can be attributed to the finer grain size in FSPed copper. Due to smaller grain size, the more grain boundaries exist in the material. Grain boundaries act as obstacles during the plastic deformation process. Further, FSPed Cu/$ZrSiO_4$ composite showed considerably higher strength than the FSPed copper which had comparable grain size. The yield strength and tensile strength of the composite was estimated to be 136±4.2 MPa and 242±3.9 MPa respectively. Whereas, it was 134±3.6 MPa and 233±4.6 MPa in case of FSPed copper. The yield and ultimate tensile strength of the fabricated Cu/$ZrSiO_4$ composite have improved

in comparison of FSPed copper. This clearly shows that apart from grain refinement zircon particle reinforcement also contributed in strength improvement. The improvement in strength of FSPed Cu/$ZrSiO_4$ composite is believed to be because of the following strengthening mechanism: As mentioned earlier, the FSP of Cu/$ZrSiO_4$ composite led to drastic grain refinement which improves the tensile strength of the composite according to famous Hall-Petch relation (Grain refinement mechanism). Secondly, the reinforced zircon particles distribution was uniform throughout the stir zone and also some of them were changed in nano-sized which acts as an obstacle for dislocation movement due to pinning effect and hence further increased the stress to overcome subsequent dislocation movement (Orowan strengthening). Thirdly, the SEM micrograph (Fig. 4.6 c) reveals that at the interface of Cu/Zircon there is no interruption i. e. no micro pores are formed and also, no other phases except copper and zircon were detected (Fig. 4.10). This means the bonding between copper and zircon particle were excellent which allow tensile load applied to be efficiently transferred from the matrix to strong zircon particles by interfacial shear strength and hence improving strength (Shear lag mechanism). Lastly, the large difference in expansion of thermal coefficients between copper and zircon sand leads to the generation of additional dislocations which further hindered the movement of dislocations and results into improved strength (thermal expansion dislocation strengthening).

The percentage elongation of the FSPed copper has improved as compared to base copper can be observed from Fig. 4.12. The improvement in ductility of FSPed copper without reinforcement with respect to base copper may be attributed to the formation of fine equiaxed grains with low dislocation density in FSPed copper, thereby leading to the improvement of work-hardening capability

(Barmouz et al., 2011a). Also, the cirtuous path to the crack propagation due to the presence of a large number of grain boundaries in FSPed copper may also contribute to enhanced plastic flow and ductility. However, the percentage elongation in case of FSPed Cu/$ZrSiO_4$ composite has decreased with respect to base copper. The reduction in ductility of the fabricated composite is attributed to higher hardness and strength due to the presence of hard zircon particle. The reinforced zircon particles resist the passage of dislocations by either creating stress field in the matrix or by inducing large differences in the elastic behaviour between the matrix and particulate (Barmouz et al., 2011b) and resulted in ductility reduction.

4.3.4.3 Fractography

Fig. 4.13 shows the fractured surfaces of the tensile tested commercially pure copper, FSPed copper with and without reinforcement.

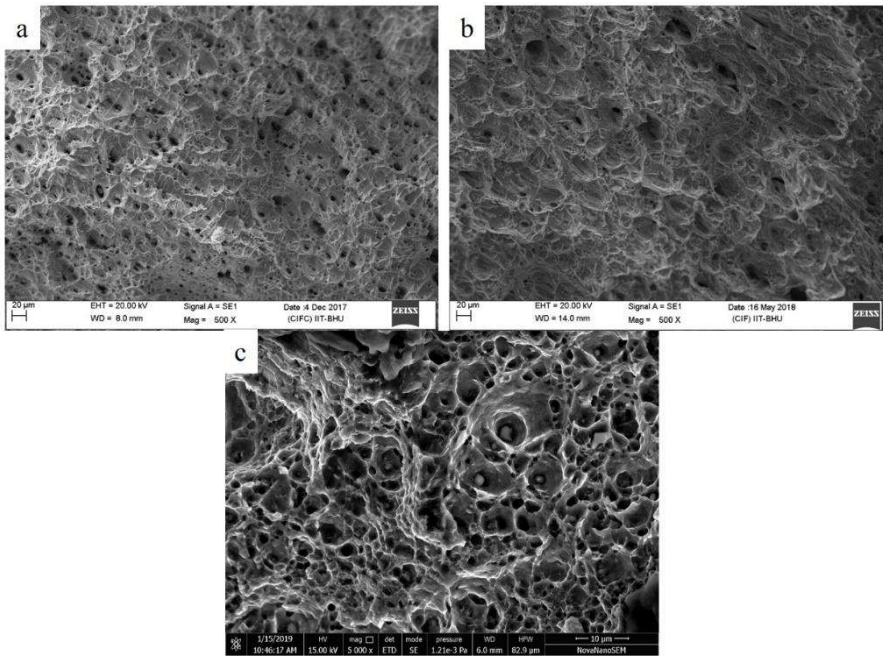

Figure 4. 13 Tensile fractographs of (a) base copper (b) FSPed copper (c) FSPed composite

The fractured surfaces of pure copper (Fig. 4.13a) resembles the typical ductile fracture characteristics i. e. deep and large dimples. The dimples in case of FSPed copper without reinforcement is slightly deeper and larger as compared to pure copper which justifies the results obtained in a tensile test. However, the dimples are narrow and shallow in case of FSPed Cu/$ZrSiO_4$ composite and getting flattened. That means the ductility of the fabricated composite has decreased as compared to pure copper. This can be attributed to their higher hardness and strength and thereby their lower ability to be deformed plastically.

4.3.5 Tribological behaviour

Fig. 4.14 shows the variation of wear loss of the Cu/zircon composite and pure copper.

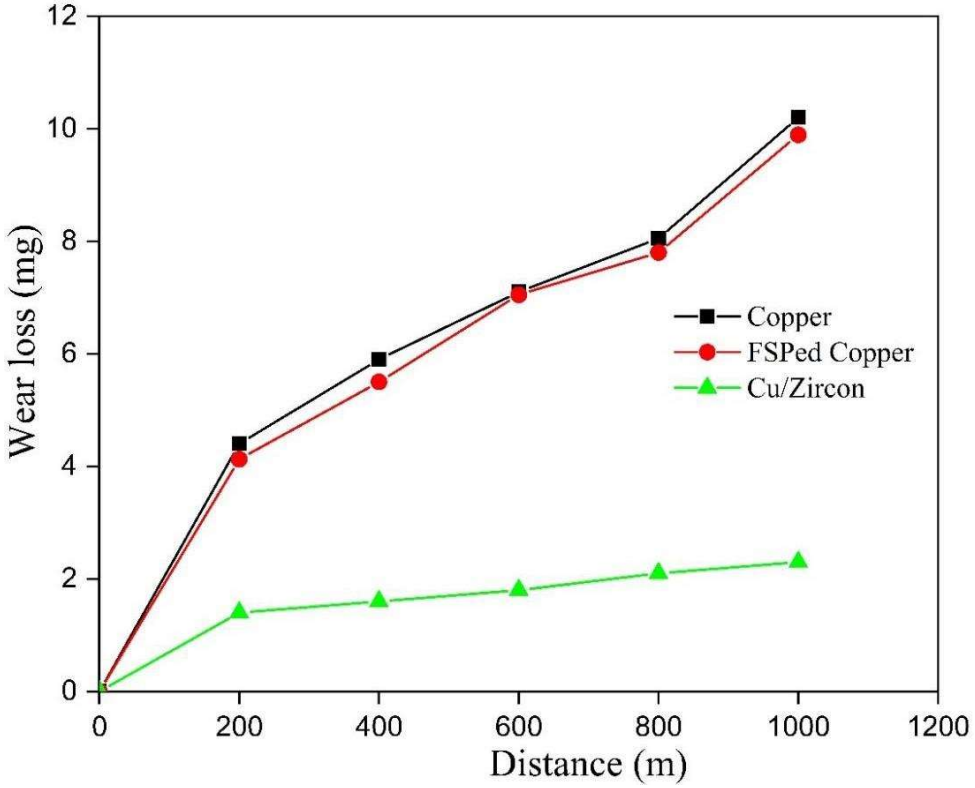

Figure 4. 14 Wear loss v/s distance profile of base copper and FSPed copper with and without reinforcement

It was observed that the wear loss was more in case of pure copper as compared to Cu/zircon composite. It can also be observed that wear resistance of FSPed copper was almost same as that of base copper which is supposed to be due to higher hardness of the processed copper. The observed wear rate of pure copper and Cu/zircon composite were $1.02x10^{-5}$ g/m and $0.23x\ 10^{-5}$ g/m respectively. The increase in wear loss exhibited almost a linear relationship with time in case of Cu/zircon composite. Fig. 4.15 shows the variation of friction coefficient of as received commercially pure copper, processed copper and Cu/zircon fabricated surface composite with time.

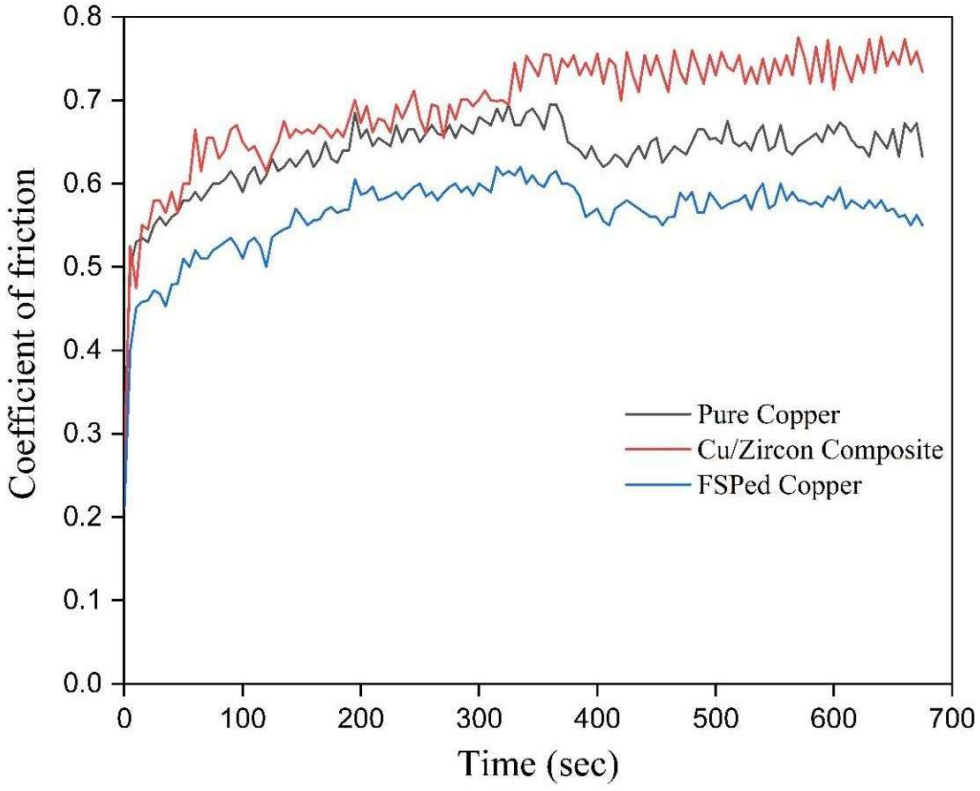

Figure 4. 15 Friction coefficient variation with time

Friction coefficient of Cu/zircon composite was observed to be higher as compared to pure copper whereas, the friction coefficient of FSPed copper is in between these two. It was also observed that the fluctuation in friction coefficient

was almost the same in the case of pure copper and fabricated composite. In the case of pure copper, it initially increased and then decreased as time progressed as can be observed from Fig. 4.15. However, in the case of Cu/zircon surface composite, friction coefficient increased first and then attained a constant value after some time. Friction coefficient of Cu/Zircon surface composite was slightly more as compared to pure copper. Incorporation of Zircon particles in copper led to an increase in abrasion resistance as the superficial hardness of composite was more as compared to pure copper. Thus resistance to sliding increased with the incorporation of Zircon particles which increased friction coefficient. In the case of pure copper, a thin tribo layer was formed on the surface of the composite and counter body due to smearing of wear debris (Barmouz et al., 2011b). But in the case of Cu/Zircon surface composite, tribo layer formation was prevented due to Zircon particles and any layer formed was abraded by Zircon particles. Thus pure copper showed less fluctuation in friction coefficient as compared to Cu/ Zircon composite. Fig. 4.15 (a) shows the SEM image of the worn surface of pure copper. Grooves resulting from ploughing effect was observed in Fig. 4.15 (a). Delamination was also observed in Fig. 4.15 (a). The surface morphology of Cu/Zircon composite was different from pure copper due to decrease in adhesion in Cu/Zircon composite. Adhesion caused delamination pits in pure copper. This led to severe material removal from the surface of pure copper. However, in the case of Cu/Zircon composite, the presence of hard Zircon particles debilitated the effect of adhesion (Zhang et al., 2006). Thus adhesive wear was very less in case of Cu/Zircon composites as was observed from Fig. 4.15 (b). The microhardness of Cu/Zircon composite was also higher as compared to pure copper which increased its resistance towards abrasive wear. It was observed in Fig. 4.15 (a) and (b) that

ploughing marks were less in Cu/Zircon composite as compared to pure Cu. The increase in abrasion resistance further reduced the wear loss of Cu/Zircon composite.

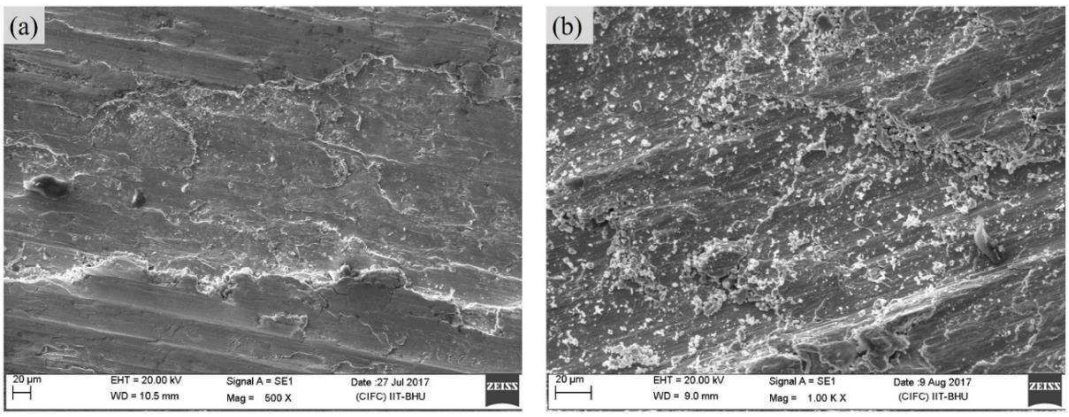

Figure 4. 16 SEM micrograph of worn surface (a) Pure Copper (b) Fabricated Composites

4.3.6 Electrical conductivity

The electrical conductivity of commercially pure copper and FSPed copper and composite was estimated to be 99.91 IACS%, 98.42 IACS%, and 74.16 IACS% respectively. It can be observed that the electrical conductivity of the composite has decreased with respect to base copper and FSPed copper without reinforcement. The electrical conductivity of FSPed copper without reinforcement is higher than the composite. The decrement in electrical conductivity of composite may be due to the presence of nonconductive zircon sand. Moreover, the decreased electrical conductivity in case of FSPed copper without reinforcement and the composite was due to more scattering of conductive electrons because of impurities, grain boundaries, surface and dislocations. As mentioned earlier, zircon reinforcement and FSP of Cu/ZrO_2 composite led to a drastic change in grain size of the copper matrix and thereby increased grain boundaries which affect the electrical conductivity of the composite. Zircon sand acted as impurities and scattering sites

for conductive electrons which affect electrical conductivity. Further, the additionally generated dislocations due to thermal mismatch also act as scattering sites for conductive electrons which affected electrical conductivity.

4.4 Conclusions

The Cu/zircon surface composite was fabricated by friction stir processing with different particle size of zircon sand. The effect of Zircon sand reinforcement on microstructure, mechanical, tribological and electrical properties were studied. The following conclusions could be drawn from the investigation:

- Copper-based surface composite was fabricated by FSP, resulted in uniform and homogeneous distribution of zircon sand.
- Frictions stir processing led to fine and equiaxed grains. The grain refinement and presence of hard zircon improved surface hardness which in turn increased the resistance to abrasion.
- The tensile strength of the FSPed copper and FSPed Cu/$ZrSiO_4$ composite improved in comparison of base copper.
- The shape and size of the reinforced zircon sand were changed due to fracture of zircon sand during processing. The sub- sized particulates dispersed uniformly in the matrix and improved the hardness of the composite further.
- Particle/matrix interface was observed to be discontinuous at some portions due to porosity. This was because of uneven shape of zircon which prevented the spread of plasticised copper and resulted in pores. However, the interruption was not observed at the interface when smaller size and even shaped zircon sand was reinforced.

- XRD pattern showed the absence of intermetallics and interfacial reaction products.
- The wear loss was less in case of Cu/zircon composite as compared to pure copper.
- The increased resistance to abrasion and adhesion led to an increase in friction coefficient in case of Cu/zircon as compared to pure copper.